AUT Journal of Electrical Engineering

AUT J. Elec. Eng., 50(1)(2018)51-58
DOI: 10.22060/eej.2017.12493.5083

Airborne Seeker Application in Three Dimensional Formation Flight of UAVs

M. A. Dehghani[1], M. B. Menhaj[1*], M. Azimi[2]

[1] Department of Electrical Engineering, Amirkabir University of Technology, Tehran, Iran
[2] Mazandaran University of Science and Technology, Behshahr, Iran

ABSTRACT: This paper deals with the leader-follower formation control problem while communication constraint in data transmitting is considered. From a practical point of view, we study the case in which unmanned vehicles are subject to the limited sensing, and communication is of a particular interest. A three-dimensional formation flight of multi-unmanned aerial vehicles with leader-follower configuration is investigated. We assume that the follower is equipped with an airborne seeker to measure the relative kinematic parameters with respect to the leader. Considering practical measurements of the airborne seeker, the kinematics of the leader-follower system is derived and by employing a cascade loop controller, the relative angle and the relative range are regulated to reach at the desired formation. Moreover, by modeling the seeker mechanism, the effect of the seeker dynamics and sensor measurement noise on the performance of the proposed formation control scheme are studied. Simulation results verify the effectiveness of the proposed leader-follower formation control structure.

Review History:
Received: 2 February 2017
Revised: 5 September 2017
Accepted: 6 September 2017
Available Online: 14 October 2017

Keywords:
Airborne seeker
Formation flight problem
Leader-Follower configuration
Unmanned Aerial Vehicles

1- Introduction

An intrinsic demand for automated, robotic and unmanned systems has largely driven by various applications such as search and rescue, fire-fighting, intelligent transportation, exploration or surveillance missions that are inherently repetitive, unpleasant, or dangerous [1]. Especially, when multiple unmanned autonomous vehicles cooperate to achieve a given task, more flexibility and robustness are accessible.

A formation of vehicles can be defined as swarming by considering some motion constraints which have been studied in three main structures, namely, leader-follower, virtual, and behavioral. The leader-follower is the most popular one in formation control due to its ease of implementation and analysis. In this structure, a vehicle is considered as a leader, and other vehicles are followers which track the leader (see [2] and references therein). In this field of research, commonly, the presence of an active communication link between the leader and the follower was assumed and the formation problem is solved based on the concept of the graph theory, e.g. see [2]-[5]. However, when the follower is only equipped with an onboard sensor to track the leader, formation control is more challenging. For instance, in [6]-[12], researchers have focused on vision-based formation control of the mobile robots using an onboard camera. Only the view-angle to the other robots is provided by each camera and the distances should be estimated [7]. Moreover, usually, a limited information exchange among the robots is assumed [9].

In the scope of formation flight problem, [13] investigates the use of line of sight (LOS) and relative measurements exchange for a relative positioning of unmanned aircraft. Tight formation flight based on visual sensory systems was studied in [14] and [15]. In these papers, the information of visual relative measurements is fused with the information of navigation sensors and global positioning system to achieve a desired relative positioning. In [16] and [17], based on LOS guidance method, the leader-follower formation flight of unmanned aircraft is studied. However, our work is distinct from the existing studies in sensor measurements specifications, and, therefore, a novel model for the leader-follower system is obtained. Absence of an active communication link between the leader and the follower is another feature that the authors of this paper pursue.

This paper is mainly intended to employ seekers as sensors that provide relative measurements for the formation keeping in the leader-follower structure. In general, seekers are categorized into two classes, namely, three axes seeker and two axes seeker [18]. In this paper, elevate-azimuth seekers which are of two-axes type and can provide relative measurements in elevation and azimuth axes are adopted. Generally, LOS angles and LOS rate angles with respect to the leader are the information provided by seekers [19]-[21]. With considering the seeker dynamics, a model for the related mechanism is accomplished. In this model, the noise of the onboard sensor in measuring the LOS angle rate is considered. In the literature, this noise is considered as the main uncertainty in seeker measurement and is called glint noise (see [22]-[27] for instance). Simulation results are given to study the effect of the seeker dynamics and sensor noise on the accuracy of the formation keeping.

It is worth mentioning that application of the proposed idea is tested by the authors via a hardware in the loop simulation test-bed in [28] and more analytical studies by considering uncertainties in seeker measurements and the leader maneuvering are presented in [29] and [30].

The rest of the paper is organized as follows. The leader-

The corresponding author; Email: menhaj@aut.ac.ir

follower kinematic equations are formulated in section 2. Modeling of the airborne seeker is presented in section 3. In section 4, the formation control structure is proposed. Section 5 provides simulation results and finally, section 6 concludes the paper.

2- leader-follower kinematic equations

Leader-follower formation can be achieved via regulation of the relative angles (ψ_{LV}, θ_{LV}) and the relative distance r_L to maintain these quantities at the desired values, as depicted in Fig. 1.

To solve the leader-follower formation problem, at first, a kinematic formulation for the follower motion equations and the leader-follower relative kinematics must be derived. For this purpose, three coordinate frames I, L and V are defined as the inertial reference frame, the line of sight frame and the follower velocity frame, respectively.

To derive the motion equations of the follower, by introducing ${}^{V}V_F = \begin{bmatrix} v_F & 0 & 0 \end{bmatrix}^T$ as the follower velocity vector V_F with respect to the frame V, we have

$$
{}^{I}V_F = {}^{I}_{V}C\,{}^{V}V_F = \begin{bmatrix} v_F \cos\psi_V \cos\theta_V \\ v_F \sin\psi_V \cos\theta_V \\ -v_F \sin\theta_V \end{bmatrix}, \tag{1}
$$

where ${}^{I}_{V}C$ denotes rotation matrix of I with respect to V; v_F is the follower speed. The variables ψ_V and θ_V are the angles of follower velocity vector with respect to the reference frame.

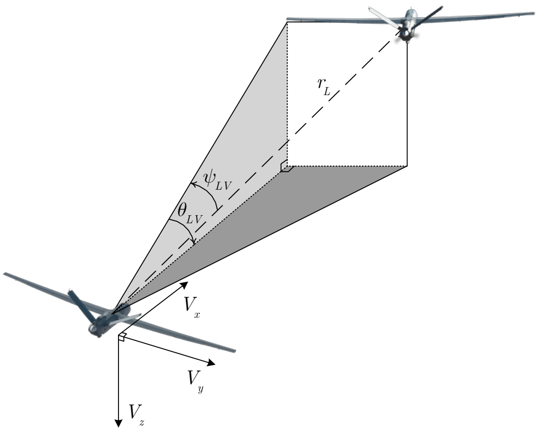

Fig. 1.The leader-follower relative kinematics.

Now, let us define $\begin{bmatrix} a_{xV} & a_{yV} & a_{zV} \end{bmatrix}^T$ as the acceleration components in the frame V. Then, $D_I V_F$ as the derivative of V_F is expressed in term of the frame I, ${}^{V}\Omega_{IV} = \begin{bmatrix} \omega_{xv} & \omega_{yv} & \omega_{zv} \end{bmatrix}^T$ as the angular velocity components in the frame V and using the following Coriolis formula,

$$
\begin{aligned}
{}^{V}D_I V_F &= \begin{bmatrix} a_{xV} \\ a_{yV} \\ a_{zV} \end{bmatrix} = D_V\,{}^{V}V_F + {}^{V}\Omega_{IV} \times {}^{V}V_F \\
&= \begin{bmatrix} \dot{v}_F \\ 0 \\ 0 \end{bmatrix} + \begin{bmatrix} \omega_{xv} \\ \omega_{yv} \\ \omega_{zv} \end{bmatrix} \times \begin{bmatrix} v_F \\ 0 \\ 0 \end{bmatrix} = \begin{bmatrix} \dot{v}_F \\ \omega_{zv} v_F \\ -\omega_{yv} v_F \end{bmatrix},
\end{aligned}
$$

in combination with (1), the motion equation of the follower can be obtained as it follows,

$$
\begin{cases}
\dot{x}_F = v_F \cos\psi_V \cos\theta_V, \\
\dot{y}_F = v_F \sin\psi_V \cos\theta_V, \\
\dot{z}_F = -v_F \sin\theta_V, \\
\dot{v}_F = a_{xV}, \\
\omega_{zv} = \dfrac{a_{yV}}{v_F}, \\
\omega_{yv} = -\dfrac{a_{zV}}{v_F},
\end{cases} \tag{2}
$$

where $\begin{bmatrix} x_F & y_F & z_F \end{bmatrix}^T$ is position vector of the follower with respect to the reference frame.

To formulate the leader-follower relative kinematics, by defining ${}^{L}R_L = \begin{bmatrix} r_L & 0 & 0 \end{bmatrix}^T$ and ${}^{L}\Omega_{IL} = \begin{bmatrix} \omega_{xl} & \omega_{yl} & \omega_{zl} \end{bmatrix}^T$, we have

$$
{}^{L}D_I R_L = \begin{bmatrix} v_{xL} \\ v_{yL} \\ v_{zL} \end{bmatrix} = {}^{L}D_L\,R_L + {}^{L}\Omega_{IL} \times {}^{L}R_L = \begin{bmatrix} \dot{r}_L \\ r_L \omega_{zl} \\ -r_L \omega_{yl} \end{bmatrix}.
$$

Time derivative of the above equation yields

$$
\begin{aligned}
{}^{L}D_I^2 R_L &= \begin{bmatrix} a_{xL} \\ a_{yL} \\ a_{zL} \end{bmatrix} = {}^{L}D_L\,{}^{L}\left(D_I R_L\right) + {}^{L}\Omega_{IL} \times {}^{L}D_I R_L \\
&= \begin{bmatrix} \ddot{r}_L - r_L\left(\omega_{yl}^2 + \omega_{zl}^2\right) \\ 2\dot{r}_L \omega_{zl} + r_L \dot{\omega}_{zl} + r_L \omega_{xl}\omega_{yl} \\ -2\dot{r}_L \omega_{yl} - r_L \dot{\omega}_{yl} + r_L \omega_{xl}\omega_{zl} \end{bmatrix},
\end{aligned}
$$

where $\begin{bmatrix} a_{xL} & a_{yL} & a_{zL} \end{bmatrix}^T$ is the LOS acceleration with respect to the frame L. Hence, by rearranging the above equation, the relative kinematic equation can be obtained as,

$$
\begin{cases}
\ddot{r}_L = r_L\left(\omega_{yl}^2 + \omega_{zl}^2\right) + a_{xL}, \\
\dot{\omega}_{zl} = -2\dfrac{\dot{r}_L}{r_L}\omega_{zl} + \dfrac{a_{yL}}{r_L} - \omega_{xl}\omega_{yl}, \\
\dot{\omega}_{yl} = -2\dfrac{\dot{r}_L}{r_L}\omega_{yl} - \dfrac{a_{zL}}{r_L} + \omega_{xl}\omega_{zl}.
\end{cases} \tag{3}
$$

Equations (2) and (3) describe the leader-follower system kinematics.

3- Airborne Seeker Modeling

In this section, a mathematical model for seeker dynamics and kinematics is expressed. A typical gimbaled seeker contains a two-degree-of-freedom gimbal in which the external gimbal is fixed to the body as shown is Fig. 2.

To derive kinematic equations, rotation matrix ${}^{S}_{V}C$ is considered as follows:

$$
\begin{aligned}
{}^{S}_{V}C &= C_3\left(\psi_{SV}\right) C_2\left(\theta_{SV}\right) \\
&= \begin{bmatrix} \cos\psi_{SV}\cos\theta_{SV} & -\sin\psi_{SV} & \cos\psi_{SV}\sin\theta_{SV} \\ \sin\psi_{SV}\cos\theta_{SV} & \cos\psi_{SV} & \sin\psi_{SV}\sin\theta_{SV} \\ -\sin\theta_{SV} & 0 & \cos\theta_{SV} \end{bmatrix}.
\end{aligned}
$$

Defining ${}^{G}\Omega_{IG} = \begin{bmatrix} \omega_{xg} & \omega_{yg} & \omega_{zg} \end{bmatrix}^T$ and ${}^{S}\Omega_{IS} = \begin{bmatrix} \omega_{xs} & \omega_{ys} & \omega_{zs} \end{bmatrix}^T$ as angular rate vectors. Now, using the following equation,

$$
\begin{aligned}
{}^{S}\Omega_{IS} &= {}^{S}_{G}C\,{}^{G}\Omega_{IG} + {}^{S}\Omega_{GS},\\
{}^{G}\Omega_{IG} &= {}^{G}_{V}C\,{}^{V}\Omega_{IV} + {}^{G}\Omega_{VG},
\end{aligned}
$$

we have

$$
\begin{cases}
\omega_{xs} = \omega_{xg}\cos\psi_{SV} - \omega_{yg}\sin\psi_{SV},\\
\omega_{ys} = \omega_{xg}\sin\psi_{SV} + \omega_{yg}\cos\psi_{SV},\\
\omega_{zs} = \omega_{zg} - \dot{\psi}_{SV},
\end{cases}
\tag{4}
$$

where

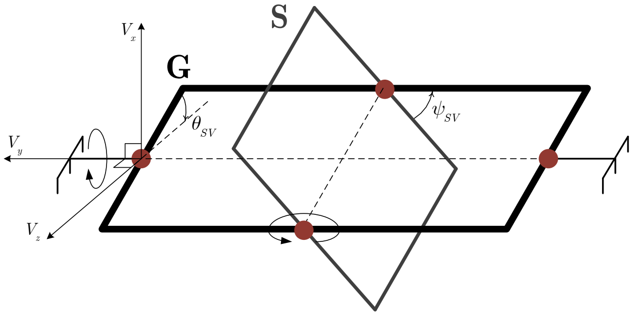

Fig. 2. Structure of two-degree-of-freedom gimbal.

$$
\begin{cases}
\omega_{xg} = \omega_{xv}\cos\theta_{SV} + \omega_{zv}\sin\theta_{SV},\\
\omega_{yg} = \omega_{yv} - \dot{\theta}_{SV},\\
\omega_{zg} = -\omega_{xv}\sin\theta_{SV} + \omega_{zv}\cos\theta_{SV}.
\end{cases}
$$

Moreover, the internal gimbal torque can be expressed as it follows,

$$
T_z = I_s\dot{\omega}_{zs} = T_{zg} + T_{zf} = T_{zg} + c_z\dot{\psi}_{SV},
\tag{5}
$$

where I_s is the moment of inertia of the internal gimbal and T_{sf} is the friction torque of the internal gimbal. Now, by using (4) in (5), one can obtain that

$$
\begin{aligned}
I_s\ddot{\psi}_{SV} + c_z\dot{\psi}_{SV} &= -T_{zg} + I_s\big[-\dot{\omega}_{xv}\sin\theta_{SV} + \dot{\omega}_{zv}\cos\theta_{SV}\\
&\quad - \dot{\theta}_{SV}\left(\dot{\omega}_{xv}\cos\theta_{SV} + \dot{\omega}_{zv}\sin\theta_{SV}\right)\big].
\end{aligned}
\tag{6}
$$

In a similar manner, for the external gimbal, we have

$$
\begin{aligned}
T_y &= \left(I_s + I_g\right)\dot{\omega}_{yg} + I_s\omega_{xg}\dot{\psi}_{SV}\\
&= T_{yg} + T_{yf} = T_{yg} + c_y\dot{\theta}_{SV},
\end{aligned}
$$

where I_g is the moment of inertia of the external gimbal. Consider the equation (4). Then, it holds that

$$
\begin{aligned}
\left(I_s + I_g\right)\ddot{\theta}_{SV} + c_y\dot{\theta}_{SV} &= -T_{yg} + \left(I_s + I_g\right)\dot{\omega}_{yv}\\
&\quad + I_s\dot{\psi}_{SV}\left(\omega_{xv}\cos\theta_{SV} + \omega_{zv}\sin\theta_{SV}\right).
\end{aligned}
\tag{7}
$$

The above-mentioned equations describe the kinematics and the dynamics of the seeker mechanism. For the sensor measurement by considering (ψ_{SL},θ_{SL}) as the seeker beam angles with respect to the leader, we have

$$
{}^{L}\Omega_{IL} = \begin{bmatrix}\omega_{xl}\\ \omega_{yl}\\ \omega_{zl}\end{bmatrix} = {}^{L}\Omega_{IS} + {}^{L}\Omega_{SL} = {}^{L}_{S}C\,{}^{S}\Omega_{IS} + {}^{L}\Omega_{SL}
$$

$$
= \begin{bmatrix}
\omega_{xs}\cos\psi_{SL}\cos\theta_{SL} + \omega_{ys}\sin\psi_{SL}\cos\theta_{SL} - \omega_{zs}\sin\theta_{SL}\\
-\omega_{xs}\sin\psi_{SL} + \omega_{ys}\cos\psi_{SL}\\
\omega_{xs}\cos\psi_{SL}\sin\theta_{SL} + \omega_{ys}\sin\psi_{SL}\sin\theta_{SL} + \omega_{zs}\cos\theta_{SL}
\end{bmatrix}
+ \begin{bmatrix}
-\dot{\psi}_{SL}\sin\theta_{SL}\\
\dot{\theta}_{SL}\\
\dot{\psi}_{SL}\cos\theta_{SL}
\end{bmatrix}.
$$

Moreover, glint noise in angle measurements is assumed and modeled as follows [22],

$$
\begin{aligned}
p(x) &= (1-\varepsilon)\,p_{G_1} + \varepsilon p_{G_2},\\
p_{G_1} &\sim N\left(0,\sigma_1^2\right),\\
p_{G_2} &\sim N\left(0,\sigma_2^2\right).
\end{aligned}
$$

This model is a mixture distribution where $p_{G_1} \sim N\left(0,\sigma_1^2\right)$ and $p_{G_2} \sim N\left(0,\sigma_2^2\right)$ are zero-mean Gaussian distributions with different standard deviations with the assumption of $\sigma_2 > \sigma_1$; ε represents the glint probability.

The achieved models for yaw and pitch channels of the airborne seeker are depicted in Fig. 3 and Fig. 4. By considering the kinematics as in (4) and the dynamics as in (6) and (7), the external inputs w_{yaw}, w_{pitch}, d_{yaw} and d_{pitch} can be formulated as follows,

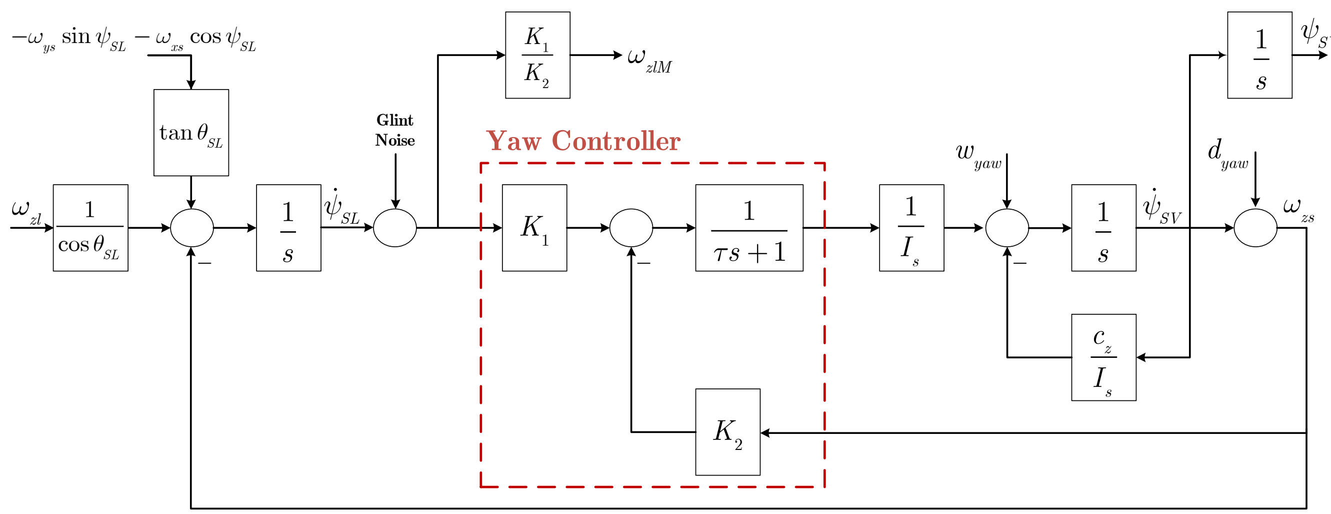

Fig. 3.Block diagram of seeker model in yaw channel

$$
\begin{aligned}
w_{yaw} &= -\dot{\theta}_{SV}\left(\omega_{xv}\cos\theta_{SV} + \omega_{zv}\sin\theta_{SV}\right) \\
&\quad + \left(\dot{\omega}_{zv}\cos\theta_{SV} - \dot{\omega}_{xv}\sin\theta_{SV}\right), \\
w_{pitch} &= \frac{I_s}{I_s + I_g}\dot{\psi}_{SV}\left(\omega_{xv}\cos\theta_{SV} + \omega_{zv}\sin\theta_{SV}\right) + \dot{\omega}_{yv}, \\
d_{yaw} &= -\omega_{xv}\sin\theta_{SV} + \omega_{zv}\cos\theta_{SV}, \\
d_{pitch} &= \omega_{xv}\sin\psi_{SV}\cos\theta_{SV} + \omega_{yv}\cos\psi_{SV} \\
&\quad + \omega_{zv}\sin\psi_{SV}\sin\theta_{SV}.
\end{aligned}
$$

In the above-mentioned models, a cascade control structure is used to control the gimbaled mechanism in the pitch and the yaw channels in which K_1, K_2, K_3 and K_4 are positive gains and τ is a time constant. This control structure is generally useful when multiple measurements with only one control variable are required for a better response to disturbances in a system. Note that the inner loop should include the major disturbances and react faster than the outer loop in order to achieve a significantly improved system performance [31].

4- FORMATION CONTROL STRUCTURE

Considering the kinematic equations presented in section 2 and the seeker model in section 3. Now, we need a control structure to complete the leader-follower formation control model. The proposed control method is a cascade loop control as follows:

$$
\begin{aligned}
a_{xL} &= k_{12}\left[k_{11}\left(r_{Ld} - r_L\right) - v_{xL}\right], \\
a_{yL} &= k_{22}\left[k_{21}\left(\psi_{LVd} - \psi_{LV}\right) - v_{yL}\right], \\
a_{zL} &= k_{32}\left[k_{31}\left(\theta_{LVd} - \theta_{LV}\right) - v_{zL}\right],
\end{aligned}
$$

where $k_{11}, k_{12}, k_{21}, k_{22}, k_{31}$ and k_{32} are positive gains that must be properly selected, and $(\psi_{LVd}, \theta_{LVd})$ and r_{Ld} are the desired values of the relative angles (orientation) and the relative distance (range). Using this control structure, the relative orientation and the relative range can be regulated to maintain these quantities at the desired values. Thus, the desired formation is achieved.

Cascade control is designed to allow the outer loop controller to respond to the slow changes in the relative distances and the relative angles, while the inner loop controller controls disturbances that happen quickly in speed or angle rates loops.

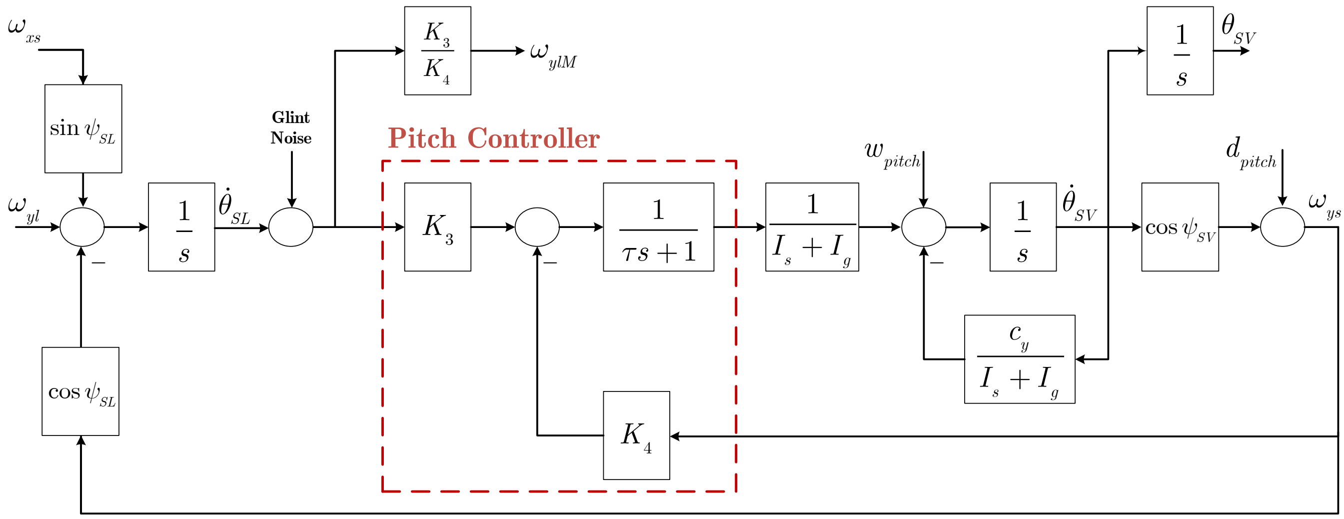

Fig. 4. Block diagram of seeker model in pitch channel

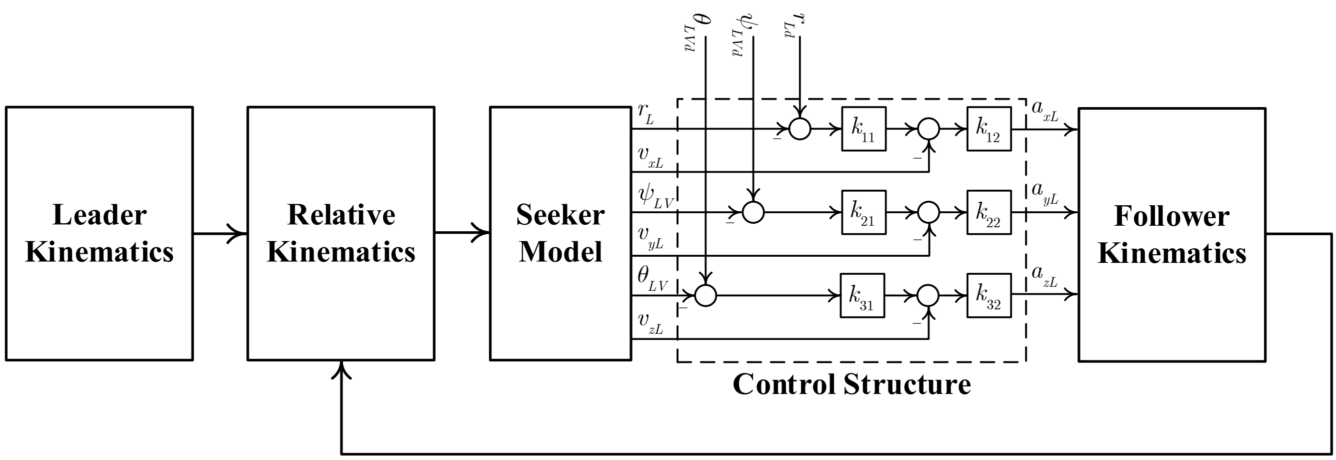

Fig. 5. Block diagram of the leader-follower formation control structure

Finally, the schematic diagram of the leader-follower formation control structure is obtained as depicted in Fig. 5. This model can be used to simulate the leader-follower formation in a proper simulation environment.

5- simulation results

In order to verify the effectiveness of the proposed control structure, a simulation is carried out for a V-shaped leader-follower formmation of three UAVs. Simulation parameters are set as listed below,

$$r_{L1d} = r_{L2d} = 250, \theta_{LV1d} = \theta_{LV2d} = -30^\circ;$$
$$\psi_{LV1d} = -45^\circ, \psi_{LV2d} = 45^\circ;$$
$$K_1 = K_3 = 1000, K_2 = K_4 = 200;$$
$$\sigma_1 = 5, \sigma_2 = 0.5, \varepsilon = 0.3;$$
$$I_g = 0.02\,\mathrm{kg.m}^2,\ I_s = 0.01\,\mathrm{kg.m}^2;$$
$$\tau = 0.1, c_z = c_y = 1;$$
$$k_{11} = 0.5, k_{12} = 1;$$
$$k_{21} = 50, k_{22} = 1;$$
$$k_{31} = 50, k_{32} = 1.$$

The initial conditions of UAVs position, speed and angles are given in Table 1.

Simulation results for 3D trajectories of the leader and followers are depicted in Fig. 6. The regulation of relative distances and angles to the desired values are shown in Fig. 7 that verify the formation achievement. Moreover, Fig. 8 to Fig. 11 evaluate the accuracy of the model of the seeker, where the measured angles and the angle rates of seekers are compared with kinematical values. We can conclude that the seeker dynamics is highly fast and, thus, does not seriously affect the accuracy of the formation. However, if a close formation (low relative distance) is intended, a filtering method should be used in the angle rate measurements.

Table 1. Initial conditions of UAVs

UAVs	Position $(x, y, z)[m]$	Speed $[m/s]$	Angles (ψ, θ)[deg]
Leader	$(250, 150, -100)$	50	$(30, 20)$
Follower1	$(0, 0, 0)$	20	d_{pitcl}
Follower2	$(100, 20, 0)$	20	$(0, 0)$

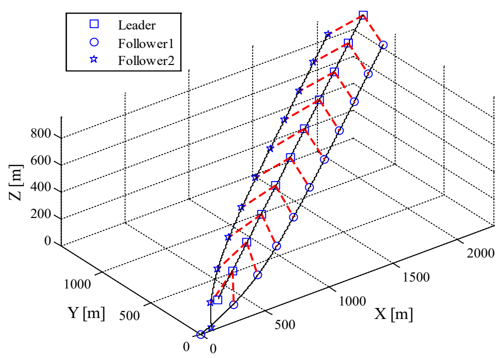

Fig. 6. The leader-follower 3D trajectories.

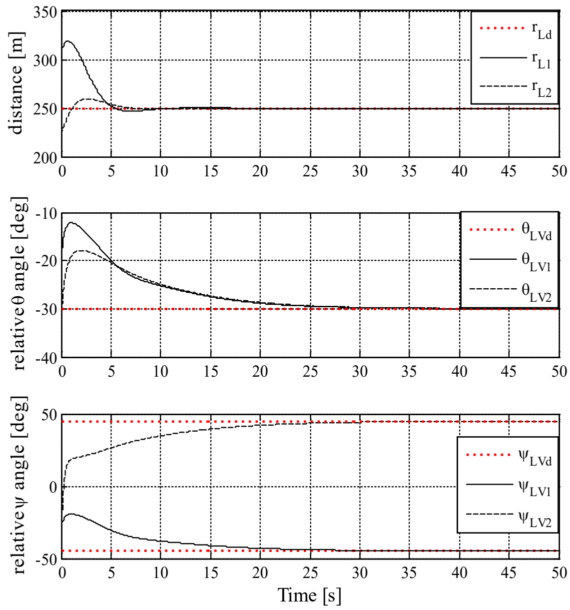

Fig. 7. Relative angles and distances regulation.

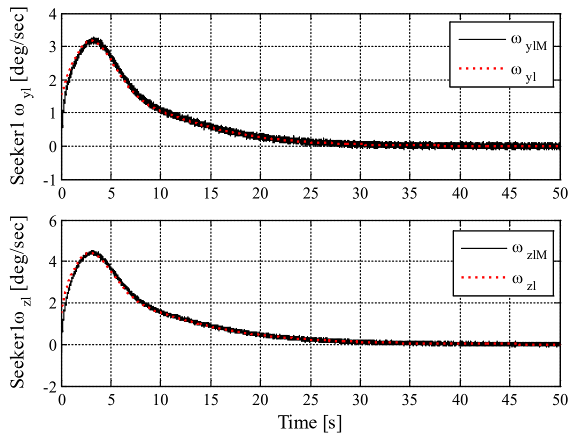

Fig. 8. Follower1 seeker angle rate measurements.

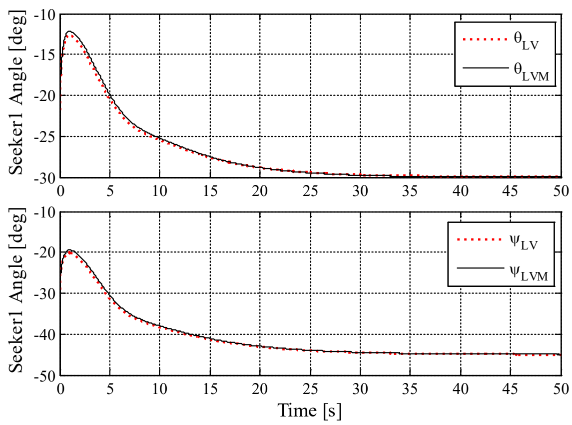

Fig. 9. Follower1 seeker angle measurements.

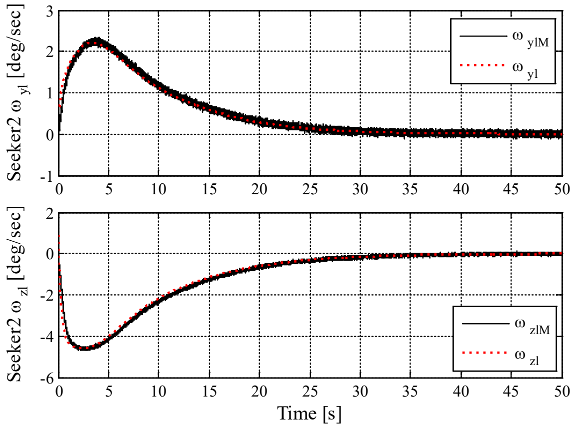

Fig. 10. Follower 2 seeker angle rate measurements.

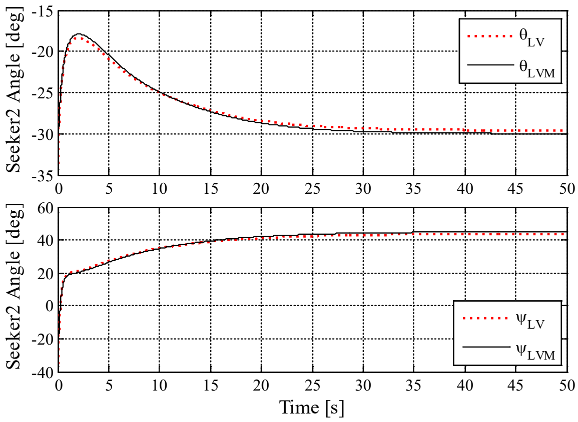

Fig. 11. Follower2 seeker angle measurements.

6- Conclusions

In this paper, a model for the leader-follower formation kinematics was proposed with considering an onboard sensor with special relative measurements. To study the effect of the airborne seeker dynamics and sensor measurement noise on the formation, the seeker mechanism was considered in the model. Then, by employing a cascade loop control structure, a proper controller was designed. Simulation results verified the application of the proposed control strategy for multi-UAV formation flight.

As for future research, one can focus on the visibility maintenance problem in which a limited field of view for the seeker will be assumed. Another potential research field is filter design to cope with measurements noises for close formation scenarios.

References

[1] A. Finn, S. Scheding, Developments and challenges for autonomous unmanned vehicles, Springer, (2010).

[2] H. Rezaee, F. Abdollahi, M. B. Menhaj, Model-free fuzzy leader-follower formation control of fixed wing UAVs, Iranian Fuzzy Systems Conference, Qazvin, Iran, (2013) 1-5.

[3] Z. Lin, W. Ding, G. Yan, C. Yu, and A. Giua, Leader follower formation via complex laplacian, Automatica, 49 (6) (2013) 1900–1906.

[4] H. Rezaee and F. Abdollahi, Motion synchronization in unmanned aircrafts formation control with communication delays, Communications in Nonlinear Science and Numerical Simulation, 18 (3) (2013) 744–756.

[5] M. Cao, A. S. Morse, C. Yu, B. D. O. Anderson, S. Dasgupta, Maintaining a directed, triangular formation of mobile autonomous agents, Communications in Information and Systems, 11 (1) (2011) 1–16.

[6] O. A. A. Orqueda, R. Fierro, A vision-based nonlinear decentralized controller for unmanned vehicles, IEEE International Conference on Robotics and Automation Orlando, Florida, (2006) 1-6.

[7] G. L. Mariottini, F. Morbidi, D. Prattichizzo, Vision based localization for leader–follower formation control, IEEE Transactions on Robotics, 25 (6) (2009) 1431-1438.

[8] B. Fidan, G. Gazi, S. Zhai, N. Cen, E. Karatas, Single view distance-estimation-based formation control of robotic swarms, IEEE Transactions on Industrial Electronics, 60 (12) (2013) 5781-5791.

[9] J. Cook, G. Hu, Z. Feng, Cooperative state estimation in vision-based robot formation control via a consensus method, 31st Chinese Control Conference, Hefei, China, (2012) 6461-6466.

[10] S. C. Liu, D. L. Tan, G. J. Liu, Robust leader-follower formation control of mobile robots based on a second order kinematics model, Acta Automatica Sinica, 33 (9) (2007) 947–955.

[11] H. J. Min, A. Drenner, N. Papanikolopoulos, Vision based leader-follower formations with limited information, in: Proceedings of the IEEE International Conference on Robotics and Automation, Kobe International Conference Center, Japan, (2009) 351– 356.

[12] G. L. Mariottini, G. Pappas, D. Prattichizzo, K. Daniilidis, Vision-based localization of leader follower formations, IEEE Conference on Decision and Control, European Control Conference, Seville, Spain, (2005) 635–640.

[13] J. Rife, Collaborative positioning for formation flight of cargo aircraft, Journal of guidance, control, and dynamics, 36 (1) (2013) 304-307.

[14] D. B. Wilson, A. H. Goktogan, S. Sukkarieh, A vision based relative navigation framework for formation flight, IEEE International Conference on Robotics and Automation, (2014) 4988–4995.

[15] Z. Mahboubi, Z. Kolter, T. Wang, G. Bower, Camera based localization for autonomous UAV formation flight, AIAA Infotech@Aerospace Conferences, Missouri, USA, (2011) 1-13.

[16] B. S. Kim, A. J. Calise, R. J. Sattigeri, Adaptive, Integrated guidance and control design for line-of sight based formation flight, Journal of Guidance, Control, and Dynamics, 30 (5) (2007) 1386- 1399.

[17] C. K. Ryoo, Y. H. Kim, M. J. Tahk, Optimal UAV formation guidance laws with timing constraint, International Journal of Systems Science, 37 (6) (2006)

415-427.

[18] H. Jiang, H. Jia, Q. Wei, Analysis of zenith pass problem and tracking strategy design for roll-pitch seeker, Aerospace Science and Technology, 23 (1) (2012) 345-351.

[19] S. Sadhu, T. K. Ghoshal, Sight line rate estimation in missile seeker using disturbance observer-based technique, IEEE Transactions on Control Systems Technology, 19 (2) (2011) 449-454.

[20] M. M. Abdo, A. R. Vali, M. R. Arvan, Improving two axes gimbal seeker performance using cascade control approach, Proceedings of the Institution of Mechanical Engineers, Part G: Journal of Aerospace Engineering, 229 (1) (2015) 38-55.

[21] M. Abdo, A. R. Vali, A. Toloei, M. R. Arvan, research on the cross-coupling of a two axes gimbal system with dynamic unbalance, International Journal of Advanced Robotic Systems, (10) (2013), 1-13.

[22] J. Kim, M. Tandale, P. K. Menon, E. Ohlmeyer, Particle filter for ballistic target tracking with glint noise, Journal of Guidance, Control, and Dynamics, 33 (6) (2010) 1918-1921.

[23] J. Waldmann, Line-of-sight rate estimation and linearizing control of an imaging seeker in a tactical missile guided by proportional navigation, IEEE Transactions on Control Systems Technology, 10 (4) (2002) 556-567.

[24] A. K. Bhattacharyya, S. Bhattacharya, T. Garai, S. Mukhopadhyay, Modeling of RF seeker dynamics and noise characteristics for estimator design in homing guidance applications, IEEE Region 10 Colloquium and the Third ICIIS, Kharagpur, INDIA, (2008) 1-7.

[25] M. R. Ananthasayanam, A. K. Sarkar, P. Vohra, A. Bhattacharya, R. Sriva Stava, Estimation of LOS rates and angles using EKF from noisy seeker measurements, International Conference on Signal Processing and Communications, (2004) 525-529.

[26] S.K. Kashyap, N. Shanthakumar, V. P. S. Naidu, G. Girija, Interacting multiple model seeker filter for homing guidance, Proceedings of ICEAE, (2009) 1-8.

[27] M. R. Ananthasayanam, A. K. Sarkar, A. Bhattacharya, P. K. Tiwari, P. Vohra, Nonlinear observer state estimation from seeker measurements and seeker radar measurements fusion, AIAA Guidance, Navigation, and Control Conference and Exhibit, San Francisco, California, (2005) 1-25.

[28] M. A. Dehghani, M. B. Menhaj, H Ghaderi, A hardware in the loop simulation testbed for vision-based leaderfollower formation flight, Mechatronics, (47) (2016) 223-232.

[29] M. A. Dehghani, M. B. Menhaj, Integral sliding mode formation control of fixed-wing unmanned aircraft using seeker as a relative measurement system, Aerospace Science and Technology, (58) (2016) 318-327.

[30] M. A. Dehghani, M. B. Menhaj, Takagi-Sugeno system for supervisory formation control of seeker mounted unmanned aerial vehicles, Assembly Automation, 36 (2) (2015) 111-119.

[31] I. Kaya, Improving performance using cascade control and a smith predictor, ISA Transactions, 40 (3) (2001) 223-234.

Please cite this article using:

M. A. Dehghani, M. B. Menhaj, M. Azimi, Airborne Seeker Application in Three Dimensional Formation Flight of UAVs, *AUT J. Elec. Eng.*, 50(1)(2018) 51-58.

DOI: 10.22060/eej.2017.12493.5083